

## Analysis of EXAFS Data from Mixed-Shell Systems

B. I. Boyanov,† G. Bunker and T. I. Morrison

Department of Physics, Illinois Institute of Technology, Chicago, IL 60616, USA

(Received 22 May 1995; accepted 13 March 1996)

A new method for analysis of EXAFS data from coordination shells containing two types of atoms distributed at two well defined distances is proposed. The method, which in effect isolates the individual contributions of the two subshells, can be viewed as a refinement of conventional techniques such as beat analysis and multi-shell least-squares fitting. No external information on the structure of any of the contributing subshells is required beyond the usual assumption of small or 'Gaussian' disorder. As much as fivefold reduction in the confidence limits of the coordination numbers in comparison with *unrestricted* multi-shell fits is demonstrated. The range of applicability and limitations of the method are discussed in detail.

**Keywords:** EXAFS; data analysis; mixed-shell analysis; beat analysis.

### 1. Introduction

Many systems of practical interest in EXAFS spectroscopy have mixed coordination shells, *i.e.* shells containing one or more types of atoms distributed at two or more unique distances differing by *ca* 0.5 Å or less. Such subshells are not resolved in the Fourier transform of the spectrum and cannot be analyzed by Fourier filtering. Methods that have been used on these systems to date include beat analysis (Martens, Rabe, Schwertner & Werner, 1977), simultaneous non-linear least-squares fitting of the subshells of interest (Sayers & Bunker, 1988) and 'difference' methods (Cramer, Eccles, Kutzler, Hodgson & Mortenson, 1976; Teo, Eisenberger, Reed, Barton & Lippard, 1978).

A typical problem with unrestricted multi-shell fits is that accurate results can usually be obtained for the bond lengths (to within 0.02 Å), but the calculated coordination numbers (CN) and their ratios are inaccurate. The relative uncertainties in the CN often exceed 100%, especially when atoms of similar scattering power and phase shifts are involved. These effects can be traced back to the strong correlation between the CN and the EXAFS Debye–Waller factors  $\sigma^2$  in the standard EXAFS equation (Sayers, Stern & Lytle, 1971), as well as to  $\Delta R$ – $\sigma^2$  correlation in systems with small bond-length differential  $\Delta R$ . Inter-shell parameter correlation, *e.g.*  $N_i$ – $N_j$  and  $\Delta R$ – $\sigma^2$  correlation, is particularly detrimental to achieving tight confidence limits for the adjustable parameters. An often-used approach to reduce these correlations and extract structural information from the data is to fix or restrict the variation of some of the parameters, *e.g.* CN ratios, Debye–Waller factors and/or edge energy. However, this requires *a priori* knowledge (usually obtained by other methods) that is not readily available in some cases.

Data with clearly manifested beats can also be analyzed by beat analysis, which gives reliable results for the bond

lengths but does not lead to any improvements in the CN estimates. 'Difference' techniques are applicable directly only in the presence of a dominant subshell. Detailed knowledge of the structure of at least one of the contributing subshells is required otherwise (Teo, 1986).

In this paper we will describe some results from a new method for EXAFS data analysis applicable to systems with subshells of atoms distributed at two well defined distances from the central absorber (Boyanov, 1995). In principle, the method may also be used to filter multiple-scattering contributions that 'contaminate' single-scattering data. The contribution of each subshell to the EXAFS spectrum is isolated through mathematical manipulations and is subsequently analyzed individually, which reduces (and in some cases eliminates) the above-mentioned parameter correlation and hence the uncertainties in the results. As usual, external information for the phase shifts of the central and backscattering atoms is required, but no assumptions are made about the structure of the subshells beyond the usual 'small' or 'Gaussian' disorder approximation, *i.e.* neglect of cumulants (Bunker, 1983) of order  $n > 2$ . This is not a serious limitation as the phase shifts can be obtained experimentally from standard compounds or calculated reliably by *ab initio* methods (Rehr, Zabinsky & Albers, 1992; Rehr, Mustre de Leon, Zabinsky & Albers, 1991).

The method has so far been tested with experimental Fe (b.c.c.), CuO (monoclinic), Fe<sub>2</sub>Zr (cubic) and Fe<sub>3</sub>O<sub>4</sub> (cubic) EXAFS data, where it has been shown to lead to improvements in CN estimates and reductions in CN confidence limits by as much as a factor of five in comparison with *unrestricted* multi-shell fits.

### 2. Theory

The total amplitude  $A$  and phase  $\varphi$  for a combination of two subshells of amplitudes and phases  $A_1, \varphi_1, A_2, \varphi_2$ , is given by  $A \exp(i\varphi) = A_1 \exp(i\varphi_1) + A_2 \exp(i\varphi_2)$ , or

† Present address: Department of Physics, North Carolina State University, Box 8202, Raleigh, NC 27695-8208, USA.

taking real and imaginary parts

$$A \cos \varphi = A_1 \cos \varphi_1 + A_2 \cos \varphi_2, \quad (1a)$$

$$A \sin \varphi = A_1 \sin \varphi_1 + A_2 \sin \varphi_2. \quad (1b)$$

This can be trivially rewritten as  $A = A_1 \exp[i(\varphi_1 - \varphi)] + A_2 \exp[i(\varphi_2 - \varphi)]$ , or taking real and imaginary parts

$$A = A_1 \cos \delta\varphi_1 + A_2 \cos \delta\varphi_2, \quad (2a)$$

$$0 = A_1 \sin \delta\varphi_1 + A_2 \sin \delta\varphi_2, \quad (2b)$$

where  $\delta\varphi_i \equiv (\varphi_i - \varphi)$ . If  $A_i$  are non-zero, (2b) implies that the nodes of  $\sin \delta\varphi_1$  and  $\sin \delta\varphi_2$  occur at the same values of  $k$ , i.e. at the nodes  $\delta\varphi_1$  and  $\delta\varphi_2$  differ by an integer multiple of  $\pi$ .

In general  $\varphi_1(k)$  and  $\varphi_2(k)$  have contributions from the central atom and backscatterer phase shifts  $\psi_i(k)$  (which are presumed known), as well as structural contributions. If both subshells have sufficiently small disorder that they can be treated as Gaussian [i.e. the cumulants (Bunker, 1983) of order  $n > 2$  are negligible], then the only relevant structural terms are  $2kR_i$ , where  $R_i$  ( $i = 1, 2$ ) are unknown and can be regarded as parameters.

In this problem,  $A$  and  $\varphi$  are known quantities that are determined experimentally. The scattering phase shifts  $\psi_i(k)$  are presumed known, so if  $R_i$  were known the phases  $\varphi_i(k) = 2kR_i + \psi_i(k)$  would be determined, and we can solve (2) for  $A_1$  and  $A_2$ :

$$A_1 = A \sin \delta\varphi_2 / \sin(\delta\varphi_2 - \delta\varphi_1), \quad (3a)$$

$$A_2 = A \sin \delta\varphi_1 / \sin(\delta\varphi_1 - \delta\varphi_2). \quad (3b)$$

The  $R_i$  values are not known precisely, but often reasonable initial guesses can be obtained (e.g. with multi-shell least-squares fitting or beat analysis). The values of  $R_i$  and the edge energy  $E_0$  may then be adjusted

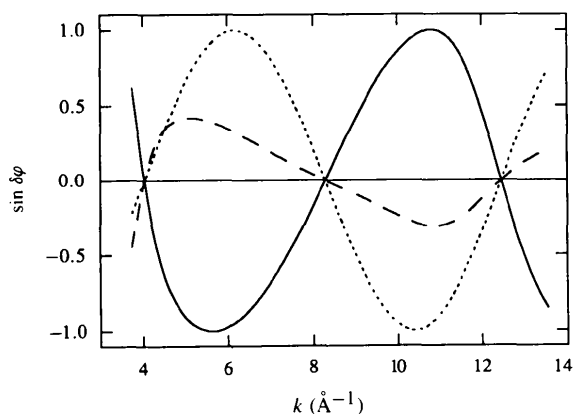


**Figure 1**  
Node-alignment procedure for metallic Fe. Solid line:  $\sin \delta\varphi_1$ ; dashed line:  $\sin \delta\varphi_2$ ; dotted line:  $\sin(\delta\varphi_2 - \delta\varphi_1)$ . The near-neighbor distances  $R_1$  and  $R_2$  and edge energy  $E_0$  are optimized simultaneously until the nodes in the phase differentials occur at the same  $k$  values.

simultaneously until the nodes of the functions  $\sin \delta\varphi_1$ ,  $\sin \delta\varphi_2$  and  $\sin(\delta\varphi_2 - \delta\varphi_1)$  are aligned, as illustrated in Fig. 1. The amplitudes  $A_1$  and  $A_2$  may then be calculated from (3), and single-shell  $\chi$  data may be obtained:

$$\chi_1(k) = A_1(k) \sin \varphi_1(k), \quad (4a)$$

$$\chi_2(k) = A_2(k) \sin \varphi_2(k). \quad (4b)$$

When suitable standards are not available for the scattering phase shifts, it will not be possible to align the nodes with the necessary precision (typically  $0.002 \text{ \AA}^{-1}$ ), and sharp 'glitches' will be present in the single-shell data calculated from (3) and (4). As long as the width of these glitches is considerably less than  $\pi/(2\Delta R)$ , where  $\Delta R = R_2 - R_1$ , they can be safely removed without any adverse effects on the quality of the results that can be obtained from the data.

As will be shown in §4, this procedure can be implemented successfully in cases of practical interest. The single-shell spectra may be subsequently fitted individually, which will be shown to result in confidence intervals for the fitting parameters that are several times smaller than those obtained with unrestricted multi-shell fits. As discussed in §1, the tightening of the confidence limits results exclusively from the elimination of the strong inter-shell parameter correlation in multi-shell fits, which is the main source of uncertainty in the fitting procedure.

### 3. Experimental methods and data processing

Four materials will be considered here: copper oxide (CuO), metallic iron (Fe), iron-zirconium intermetallic compound ( $\text{Fe}_2\text{Zr}$ ) and iron oxide ( $\text{Fe}_3\text{O}_4$ ).

The experimental data for CuO, Fe and  $\text{Fe}_2\text{Zr}$  were collected in fluorescence mode at beamline X11-A at NSLS, with an electron-beam energy of 2.528 GeV and stored currents between 110 and 240 mA. The primary X-ray beam was monochromatized with a non-dispersive variable-exit Si(111) monochromator. Energy resolution was estimated to be at least 3 eV from the copper 3d near-edge feature. Harmonics were suppressed by detuning 15% from the maximum intensity. Copper-edge data were collected at room temperature with an Ni filter, and iron-edge data were collected at liquid-nitrogen temperature with an Mn filter. All filters were approximately three absorption lengths thick. In both cases the  $I_0$  and  $I_f$  detectors were continuously flushed with  $60 \text{ cm}^3 \text{ min}^{-1}$  nitrogen and  $60 \text{ cm}^3 \text{ min}^{-1}$  argon, respectively. The CuO sample (99.99%+, Aldrich) was in the form of a 2 mm-thick self-supporting 13 mm pellet. The Fe sample was a thin film (ca 3000 Å) sputtered on a 1 mil (25.4 μm) Kapton substrate. The  $\text{Fe}_2\text{Zr}$  sample was a 10 mm-thick button.

Iron oxide ( $\text{Fe}_3\text{O}_4$ ) data were collected at room temperature in transmission mode on beamline 7-3 at SSRL in dedicated mode. The sample preparation and measurement conditions have been described previously (Bunker, 1984). The beam current and energy were 2.95 GeV and 80 mA, respectively. The primary X-ray beam was monochromatized

with a non-dispersive Si(220) monochromator. Harmonics were monitored with an NaI scintillator PMT and rejected through detuning of the monochromator crystals. The  $I_0$  and  $I$  ion chambers were continuously flushed with nitrogen. Energy calibration was set to 8980 eV at the Cu 3d edge feature and maintained with a  $\text{CoSO}_4 \cdot 7\text{H}_2\text{O}$  standard positioned in series with the sample. The sample and standard were brushed on Scotch Magic transparent tape, and six layers of tape were used to achieve a step size  $\Delta m.x \approx 0.3$ . Particle size was estimated to be less than 1  $\mu\text{m}$  (sedimentation).

McMaster corrections (McMaster, Kerr, Del Grande, Mallett & Hubbell, 1968) were calculated for all experimental  $\chi$  data. In addition, fill-gas (Bunker, 1988) and 'self-absorption' (Tan, Budnick & Heald, 1989) corrections were applied to the fluorescence data. Background subtraction and Fourier filtering were performed with the Macintosh version of the University of Washington/Naval Research Laboratory package (*MacXAFS*, Version 3.1) (Bouldin, Elam & Furenlid, 1995) in the ranges indicated in Table 1 and Fig. 2. Structural parameters were determined with non-linear least-squares fitting to the standard EXAFS equation (Sayers *et al.*, 1971) with a program written in-house. The scattering phase shifts  $\psi_i(k)$  and backscattering amplitudes  $F_i(k)$  used in the fits were calculated with *FEFF6.01a* (Rehr *et al.*, 1991, 1992) from the known crystal structures of CuO, Fe,  $\text{Fe}_2\text{Zr}$  and  $\text{Fe}_3\text{O}_4$  (Wyckoff, 1963). All crystal structures used by *FEFF* were generated by *ATOMS2.41* (Ravel, undated). Multiple-scattering effects were found to be negligible in the analyzed data ranges. Single-shell

**Table 1**

Fourier transform and fitting ranges.

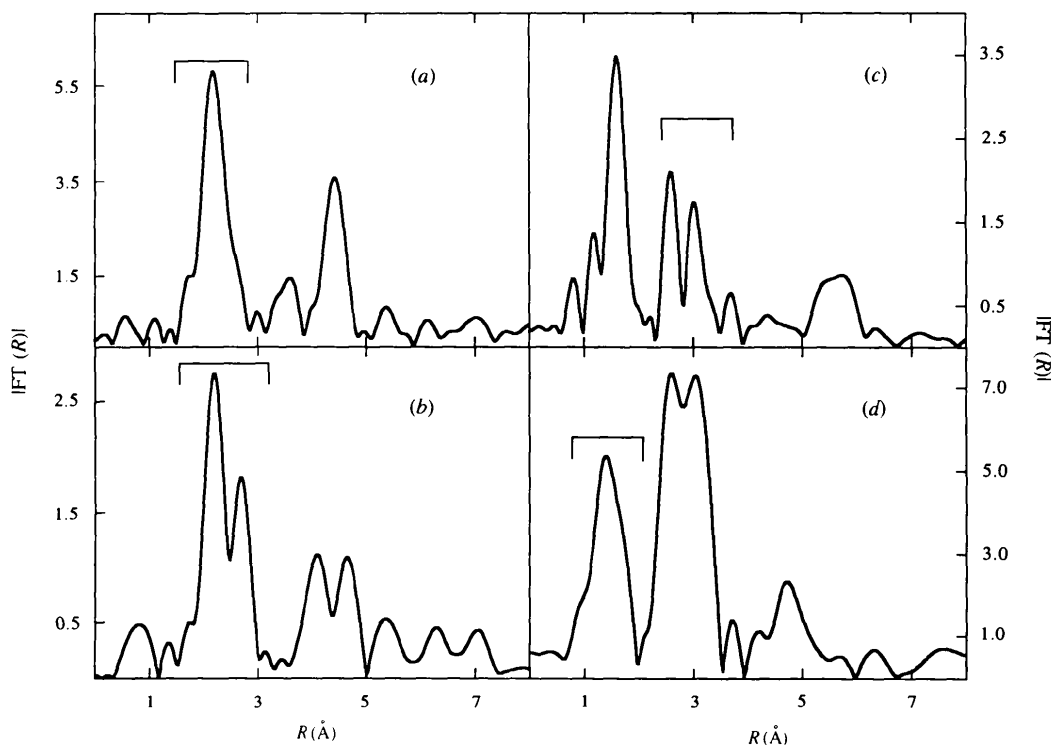
FTR = forward transform and IFTR = inverse transform. A 0.5 Å Hanning window was used in the forward transform and was divided out from the filtered data.

Sample	FTR (Å <sup>-1</sup> )	IFTR (Å)	Fit (Å <sup>-1</sup> )
Fe	2.75–14.10	1.50–2.85	3.85–13.50
$\text{Fe}_2\text{Zr}$	3.45–14.20	1.57–3.20	4.10–13.80
CuO	2.90–13.80	2.27–3.38	3.50–13.50
$\text{Fe}_3\text{O}_4$	2.60–12.00	0.74–2.00	4.15–11.15

data for the atomic pairs of interest were generated from the *FEFFnnnn.dat* files and were Fourier filtered over ranges identical to those given in Table 1 before being used in the fits. The amplitudes of the theoretical data were additionally adjusted by constant factors determined from fits to experimental data from standard compounds (Fe and Cu foil).

Unless explicitly stated otherwise, the edge energy  $E_0$ , coordination numbers  $N_i$ , bond distances  $R_i$ , and Debye–Waller factors  $\sigma_i^2$  were used as adjustable parameters. The optimization procedure was a modification of the Levenberg–Marquardt algorithm as implemented in *MINPACK-1* (More, Gabrow & Hillstom, 1980). The program minimized the quantity

$$(\Delta\chi)^2 = (1/N_{\text{pts}}) \sum_i^{N_{\text{pts}}} \left[ k_i^w (\chi_i^{\text{exp}} - \chi_i^{\text{theo}}) \right]^2, \quad (5)$$

**Figure 2**

Inverse Fourier transform ranges: (a)  $k^2$ -weighted pure iron; (b)  $k$ -weighted iron–zirconium intermetallic compound ( $\text{Fe}_2\text{Zr}$ ); (c)  $k^3$ -weighted copper oxide (CuO); (d)  $k^3$ -weighted  $\text{Fe}_3\text{O}_4$ .

**Table 2**

Structural parameters for metallic Fe.

XRD values are from Wyckoff (1963). All EXAFS coordination numbers are corrected for self absorption.

Subshell	XRD		$N$	Two-shell fit $R$ (Å)	$\sigma^2 \times 10^4$ (Å <sup>2</sup> )	$N$	$\delta\varphi$ method $R$ (Å)	$\sigma^2 \times 10^4$ (Å <sup>2</sup> )
	$N$	$R$ (Å)						
Fe-Fe <sub>1</sub>	8.0	2.49	8.1 ± 2.8	2.47 ± 0.02	22 ± 21	8.5 ± 1.9	2.48 ± 0.01	21 ± 15
Fe-Fe <sub>2</sub>	6.0	2.87	9.1 ± 7.6	2.84 ± 0.04	69 ± 66	5.2 ± 1.7	2.85 ± 0.01	50 ± 24

where  $w$  will be referred to as the weight of the fit, and  $N_{\text{pts}}$  is the number of data points in the fitting range. Confidence limits for the fitting parameters were determined from the square roots of the diagonal elements of the covariance matrix of the fit, multiplied by the value of  $\sqrt{(\Delta\chi)^2}$  at the minimum. This is equivalent to assigning an error bar to every data point equal to the r.m.s. difference between the experimental data and the best fit, and setting the minimum value of  $(\Delta\chi)^2$  to 1.0 (Press, Flannery, Teukolsky & Vetterling, 1989). The confidence limits determined in this way give the deviations of each fitting parameter from the 'optimal' values that double  $(\Delta\chi)^2$  when all other parameters are simultaneously relaxed. It should be noted that with the above definition the quoted confidence limits do *not* represent independent estimates of the uncertainties in the adjustable parameters, but are simply a measure of the sensitivity of the function  $(\Delta\chi)^2$  to small variations in these parameters, subject to the chosen normalization [equation (5)] and/or restrictions imposed on the fit.

#### 4. Examples and discussion

This section illustrates the derivations in §2 with several practical examples. The data analysis proceeds as follows:

(i) Fourier filter the data corresponding to the two subshells of interest.

(ii) Extract structural parameters from the filtered data with an unrestricted least-squares fit of the two subshells.

(iii) Isolate the contribution of each subshell according to the procedure described in §2 (hereafter referred to as the  $\delta\varphi$  method).

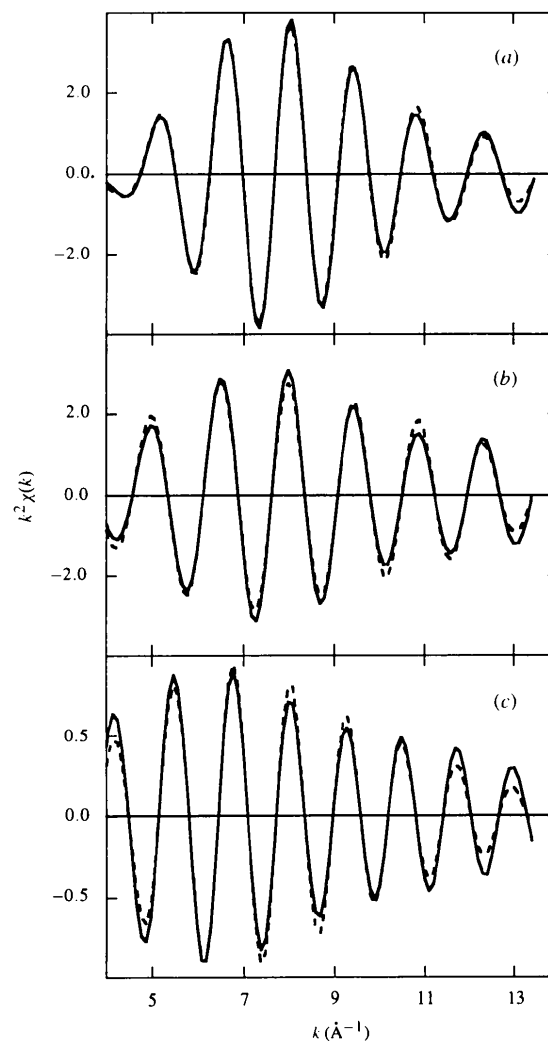
(iv) Fit each subshell individually while holding the bond distances and edge shifts fixed to the values derived from the  $\delta\varphi$  method, and compare the results with those obtained with the two-shell fit. It should be noted that the elimination of the bond lengths  $R_i$  and edge shift  $E_0$  from the fitting procedure is done solely for the sake of consistency. No degradation in the quality of the results occurs if these parameters are allowed to vary.

In all cases it was found that the  $\delta\varphi$  method gives results that are in better agreement with the known structural parameters than the *unrestricted* two-shell fits.

##### 4.1. Metallic iron

Metallic iron (Fe) has a b.c.c. structure with the first shell consisting of eight near neighbors at 2.486 Å and six near neighbors at 2.870 Å (Wyckoff, 1963). Experimental EXAFS data were Fourier transformed in the range 2.75–

14.10 Å<sup>-1</sup> and filtered in  $R$  space in the range 1.50–2.85 Å (Fig. 2). The results of a  $k^2$  unrestricted two-shell fit to the filtered data are shown in Table 2 and Fig. 3. The filtered data were also processed with the  $\delta\varphi$  method. An edge shift  $E_0 = 2.0$  eV and near-neighbor distances  $R_{1,2} = 2.459, 2.865$  Å were required to align the nodes of the phase-difference functions at  $k = 4.034, 8.293$  and  $12.452$  Å<sup>-1</sup>, as shown in Fig. 1. Almost perfect alignment of the nodes of the sine functions was possible in this case, and no visible discontinuities were present in the single-shell data. Results

**Figure 3**

Iron (b.c.c.): experimental (solid line) and fitted (dashed line) data. (a) Two-shell fit; (b) Fe-Fe<sub>1</sub> subshell; (c) Fe-Fe<sub>2</sub> subshell.

**Table 3**Structural parameters for Fe<sub>2</sub>Zr.

XRD values are from Wyckoff (1963). All EXAFS coordination numbers are corrected for self absorption.

Subshell	XRD		N	Two-shell fit R (Å)	$\sigma^2 \times 10^4$ (Å <sup>2</sup> )	N	$\delta\varphi$ method R (Å)	$\sigma^2 \times 10^4$ (Å <sup>2</sup> )
	N	R (Å)						
Fe-Fe	6.0	2.49	5.7 ± 1.2	2.49 ± 0.01	10 ± 12	6.0 ± 1.2	2.49 ± 0.01	11 ± 12
Fe-Zr	6.0	2.92	4.2 ± 2.0	2.92 ± 0.01	4 ± 21	6.0 ± 1.7	2.92 ± 0.01	17 ± 14

from single-shell fits to the  $\delta\varphi$ -filtered data are given in Table 2 and Fig. 3.

The bond distances obtained from the unrestricted two-shell fit are in agreement in the X-ray diffraction (XRD) values, but the discrepancy in the CN ratio is at least 35%, and the relative confidence limit for the Fe-Fe<sub>2</sub> subshell CN is 83%. As mentioned earlier, this is not unusual for unrestricted fits of subshells containing atoms of similar scattering power and phase shift. However, the coordination numbers and their ratio obtained with the  $\delta\varphi$  method are in agreement with the known values. In addition, the confidence interval for the Fe-Fe<sub>2</sub> subshell is reduced by a factor of five.

#### 4.2. Iron-zirconium intermetallic compound

The structure of the iron-zirconium intermetallic compound (Fe<sub>2</sub>Zr) is cubic (space group  $Fd\bar{3}m$ ) with six Fe atoms at 2.493 Å and six Zr atoms at 2.923 Å around each Fe atom (Wyckoff, 1963). Results from the unrestricted two-shell fit and the fits of the individual subshells (isolated by the  $\delta\varphi$  method) are shown in Table 3 and Fig. 4. The improvements in the  $\delta\varphi$ -method results are not as dramatic as in the previous example, but are nevertheless significant.

#### 4.3. Copper oxide

Copper oxide (CuO) has a monoclinic structure [space group  $C2/c$  (Wyckoff, 1963)], and was used 15 years ago to develop the beat-analysis method (Martens *et al.*, 1977). The first shell around each Cu atom consists of an irregular square of four O atoms at *ca* 1.95 Å from the central Cu atom. The second shell is dominated by two Cu subshells consisting of four atoms each at 2.88 and 3.07 Å, but also has contributions from two O atoms at 2.77 Å and two Cu atoms at 3.16 Å. Thus, CuO does not fall into the domain of the  $\delta\varphi$  method, but since the signal is dominated by the 2.88 and 3.07 Å Cu subshells, it may be used to test the robustness of the method. The results from an unrestricted two-shell fit are shown in Table 4 and Fig. 5. The fit quality is excellent and the bond distances are in agreement with the XRD values, but the ratio of the coordination numbers is 510% in error. The fitting results for the individual subshells (isolated by the  $\delta\varphi$  method) are shown in Table 4 and Fig. 5. The CN ratio is still more than 50% in error, and there is a clearly visible mismatch in the amplitudes of the Cu-Cu<sub>2</sub> subshell fit, which is probably due to the ignored contributions of the two Cu atoms at 3.16 Å. It is interesting to note that the results for the Cu-Cu<sub>1</sub> shell are in agreement with the XRD values.

#### 4.4. Iron oxide

Iron oxide (Fe<sub>3</sub>O<sub>4</sub>) has a cubic structure [space group  $Fd\bar{3}m$  (Wyckoff, 1963)]. Two kinds of Fe sites are present in this compound, one with four O atoms at 1.876 Å from the central Fe atom (33.3% of the sites), and a second one with six O atoms at 2.066 Å from the central atom (66.6% of the sites). This compound is interesting for several reasons. First, the bond-length differential between the subshells is only 0.19 Å, so this compound is at the lower limit of applicability of the  $\delta\varphi$  method (see §4.5). The bond

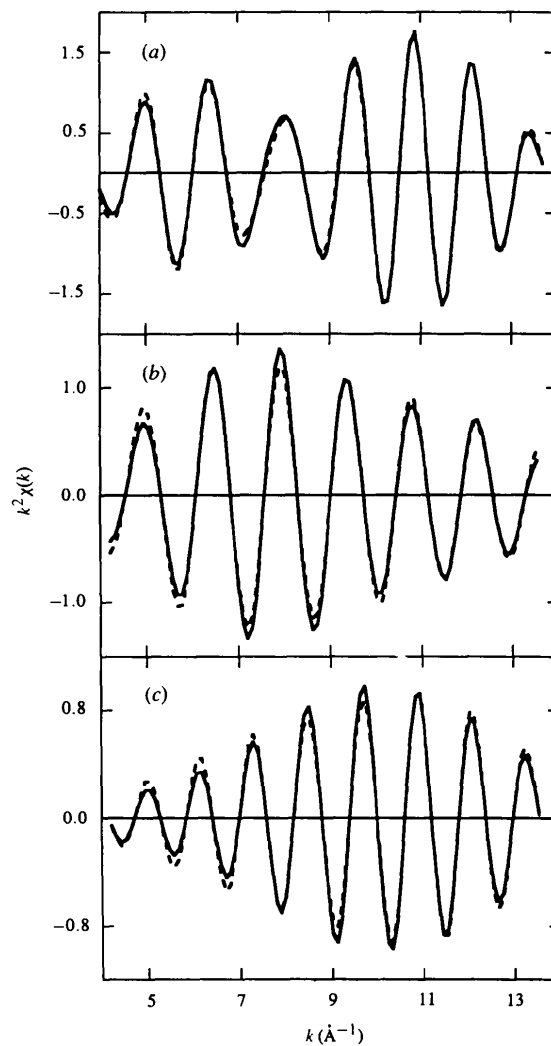


**Figure 4** Fe<sub>2</sub>Zr: experimental (solid line) and fitted (dashed line) data. (a) Two-shell fit; (b) Fe-Fe subshell; (c) Fe-Zr subshell.

**Table 4**  
Structural parameters for CuO.

XRD values are from Martens *et al.* (1977). All EXAFS coordination numbers are corrected for self absorption.

Subshell	XRD		$N$	Two-shell fit		$\sigma^2 \times 10^4$ ( $\text{\AA}^2$ )	$N$	$\delta\varphi$ method	
	$N$	$R$ ( $\text{\AA}$ )		$R$ ( $\text{\AA}$ )	$\sigma^2 \times 10^4$ ( $\text{\AA}^2$ )			$R$ ( $\text{\AA}$ )	$\sigma^2 \times 10^4$ ( $\text{\AA}^2$ )
Cu-Cu <sub>1</sub>	4.0	2.88	$10.2 \pm 3.3$	$2.93 \pm 0.01$	$50 \pm 45$	$3.7 \pm 1.7$	$2.90 \pm 0.00$	$51 \pm 27$	
Cu-Cu <sub>2</sub>	4.0	3.07	$2.0 \pm 1.3$	$3.14 \pm 0.01$	$8 \pm 26$	$2.4 \pm 1.5$	$3.10 \pm 0.01$	$24 \pm 31$	

**Table 5**  
Structural parameters for Fe<sub>3</sub>O<sub>4</sub>.

XRD values are from Wyckoff (1963). Two-shell results are obtained from 'restricted' fits with  $\sigma_{1,2}^2$  held fixed at 0.0010 and 0.0020  $\text{\AA}^2$ , respectively.

Subshell	XRD		$N$	Two-shell fit		$\sigma^2 \times 10^4$ ( $\text{\AA}^2$ )	$N$	$\delta\varphi$ method	
	$N$	$R$ ( $\text{\AA}$ )		$R$ ( $\text{\AA}$ )	$\sigma^2 \times 10^4$ ( $\text{\AA}^2$ )			$R$ ( $\text{\AA}$ )	$\sigma^2 \times 10^4$ ( $\text{\AA}^2$ )
Fe <sub>1</sub> -O	1.3	1.88	$2.6 \pm 1.0$	$1.88 \pm 0.06$	—	$1.3 \pm 0.5$	$1.89 \pm 0.02$	$10 \pm 15$	
Fe <sub>2</sub> -O	4.0	2.07	$3.8 \pm 1.3$	$2.02 \pm 0.06$	—	$2.9 \pm 1.0$	$2.03 \pm 0.02$	$20 \pm 20$	

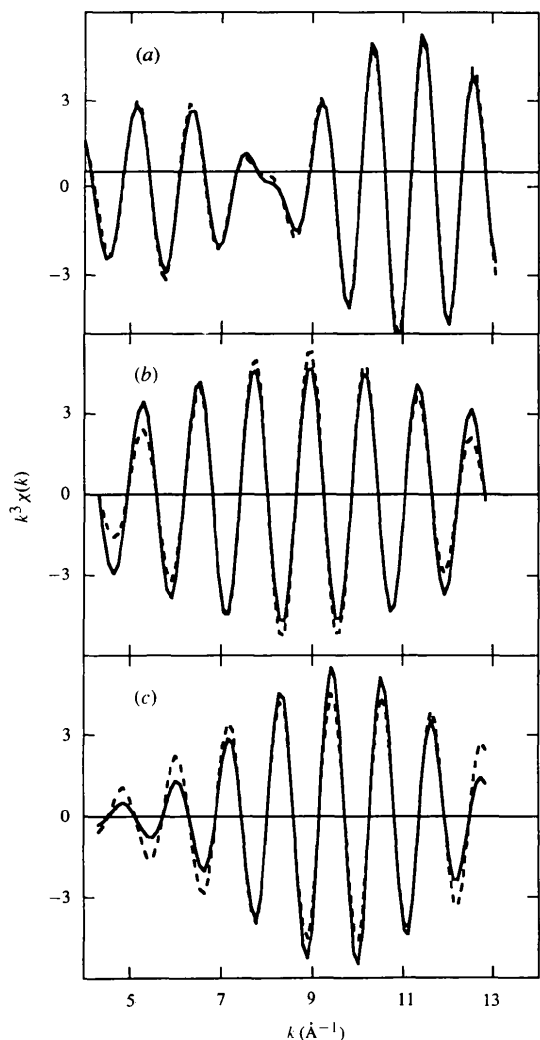


**Figure 5**  
Copper oxide (CuO) fitting results: experimental (solid line) and fitted (dashed line) data. (a) Two-shell fit; (b) Cu-Cu<sub>1</sub> subshell; (c) Cu-Cu<sub>2</sub> subshell.

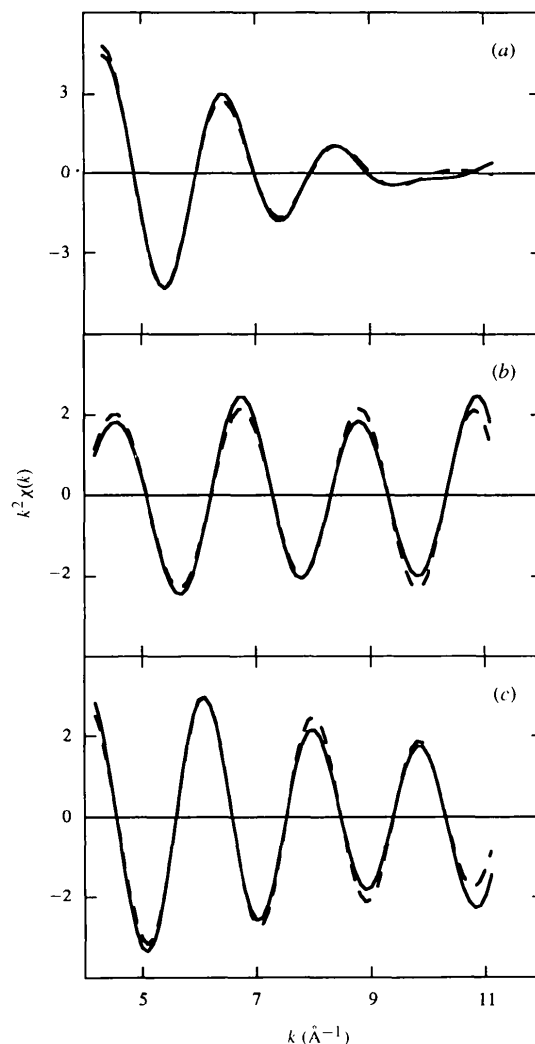


**Figure 6**  
Iron oxide (Fe<sub>3</sub>O<sub>4</sub>) fitting results: experimental (solid line) and fitted (dashed line) data. (a) Two-shell fit; (b) Fe<sub>1</sub>-O subshell; (c) Fe<sub>2</sub>-O subshell.

distances in the first shell are also substantially shorter than in the other model compounds used in this study, and thus the effects of the background on the results potentially can be evaluated. Unrestricted two-shell fits of the filtered data were completely unreliable due to the additional strong correlations between the distance differential  $\Delta R$  and the Debye–Waller factors of the subshells. In order to restrict this correlation and obtain some structural information from the two-shell fits, the Debye–Waller factors were not allowed to vary during the optimization. The results of this restricted fit are shown in Table 5 and Fig. 6, and are in agreement with the known structural parameters. The fitting results for the individual subshells (isolated with the  $\delta\varphi$  method) are also given in Table 5 and Fig. 6. The bond distances are in agreement with the XRD values, even though no additional restrictions were imposed in the fits. The source of the observed discrepancies in the coordination numbers is discussed below.

#### 4.5. Range of applicability and limitations

The spatial resolution of the  $\delta\varphi$  method is determined from the requirement that the  $\sin(\delta\varphi_i)$  functions have at least one node in the data range of interest, which may also be written as

$$2k(R_2 - R_1) + [\psi_2(k) - \psi_1(k)] = m\pi, \quad (6)$$

where  $m = 0, \pm 1, \pm 2, \dots$ . Here,  $\psi_i(k)$  ( $i = 1, 2$ ) are the scattering phase shifts for the two subshells. Equation (6) must be satisfied for at least one  $k$  in the range  $k_{\min}, k_{\max}$ , and may be compared with the equation for the positions of the beats in the amplitude of the two-shell data (Martens *et al.*, 1977):

$$2k(R_2 - R_1) + [\psi_2(k) - \psi_1(k)] = (2n + 1)\pi, \quad (7)$$

where  $n = 0, \pm 1, \pm 2, \dots$ . It is clear that two nodes are present for every beat in the amplitude function. When the backscattering atoms are similar or identical [ $\psi_1(k) \simeq \psi_2(k)$ ], the first beat and the first node occur at the same  $k$  value ( $\pi/2\Delta R$ ), and the spatial resolutions of the beat analysis and  $\delta\varphi$  methods are identical, *ca* 0.15 Å. However, if the two backscatterers are different, (6) is dominated by the term  $2k\Delta R$ , but the term  $\psi_2(k) - \psi_1(k)$  may have a non-negligible magnitude and  $k$  dependence. In particular, the  $\Delta\psi(k)$  term will cause a node in the phase-difference function (6) at a *lower*  $k$  value than the first beat in the spectrum. If this node is in the usable part of the spectrum (*i.e.* above  $k_{\min}$ ), the  $\delta\varphi$  method will have higher spatial resolution than beat analysis. Equation (6) may thus be used to determine the spatial resolution of the  $\delta\varphi$  method on a case-by-case basis, *e.g.* with tabulated or *ab initio* scattering phase shifts.

Since all trigonometric functions have many zeroes, there is no reason to expect that the node-alignment procedure leads to a unique solution for  $R_i$ . On the contrary, it is quite possible that multiple solutions exist. If, for example,

the node-alignment criterion is satisfied at a node  $k_0$  for some particular  $R_i$ , it will also be satisfied at  $k_0$  for  $R_i + n_i\pi/2k_0$  ( $n_i = 0, \pm 1, \pm 2 \dots$ ) [see (6)]. Fortunately, the term  $n_i\pi/k_0$  depends on the position of the node  $k_0$ , so that if two or more nodes are present in the data range, multiple solutions will exist only if the ratio of *any* two node positions can be expressed as a fraction of the form  $m/n$ , with  $m$  and  $n$  small integers. This can be done with arbitrary accuracy for large values of  $m$  and  $n$ , but these will lead to large or negative  $R_i$ , which can easily be ruled out, *e.g.* on the basis of results obtained from a two-shell fit. However, when single-shell data are isolated through the alignment of a single node, there is no direct way of distinguishing the spurious solutions from the ‘true’ one, and external information must be used. For example, with metallic iron (see §4.1) it was possible to align the nodes at  $k = 4.034, 8.293$  and  $12.452 \text{ \AA}^{-1}$  with an edge shift of 2.0 eV and  $R_{1,2} = 2.459, 2.865 \text{ \AA}$ , and at  $k = 6.959 \text{ \AA}^{-1}$  with an edge shift of  $-7.6$  eV and  $R_{1,2} = 2.632, 2.882 \text{ \AA}$ . The  $\delta\varphi$  method therefore suffers from the same potential problem of multiple local minima as does ordinary non-linear least-squares fitting. It must be noted that since the edge energy  $E_0$  is also varied in the fit, the multiple solutions, whenever present, are not discrete. Single-node solutions can always be ignored in favor of multi-node solutions, but in the absence of additional information the only way to distinguish two single-node solutions with physically reasonable  $R_i$  may be the shape of the amplitude functions. In the case of metallic Fe, the single-node solution had a clearly visible beat in the vicinity of  $10 \text{ \AA}^{-1}$ , while the backscattering function of Fe is known to be decreasing monotonically in this  $k$  range.

The accuracy of the results that can be obtained from the  $\delta\varphi$  method may be limited by the presence of multiple local minima. Distance differentials at the low end of applicability of the method (*e.g.* 0.15–0.20 Å for similar scatterers) will result in only a single node within the fitting range which, as noted at the beginning of this

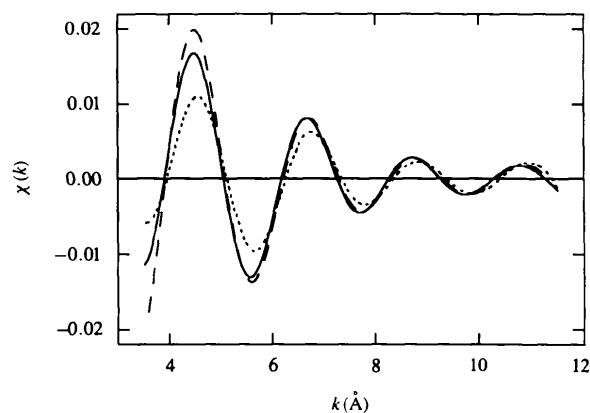


**Figure 7**

Dependence of the first-shell iron oxide ( $\text{Fe}_3\text{O}_4$ ) data on the node position:  $k_0 = 10.236 \text{ \AA}^{-1}$  (solid line);  $k_0 = 10.013 \text{ \AA}^{-1}$  (dashed line);  $k_0 = 10.106 \text{ \AA}^{-1}$  (dotted line).

section, is undesirable. This appears to be the source of the discrepancy between the  $\delta\varphi$  and XRD coordination numbers for  $\text{Fe}_3\text{O}_4$  and the somewhat large error bars in the results. Since the distance differential for this material is 0.15–0.18 Å, only a single node at approximately  $10 \text{ \AA}^{-1}$  was present in the fitting range, and its position was found to vary by as much as  $0.25 \text{ \AA}^{-1}$  with the initial guesses used in the node-alignment procedure. The bond lengths appear to be independent (within the confidence limits) of such variations in the node position, but the CN and Debye–Waller factors are more sensitive, as shown in Fig. 7. Therefore, we expect that the practical lower limit on the resolvable distance differential for similar/identical scatterers is probably closer to 0.25–0.30 Å if accurate data for the coordination numbers are also required.

The sensitivity of the amplitude functions of the filtered data to variations in the node positions raises the concern that results of the method may be dependent on the details of the background subtraction. We have conducted tests with the Fe,  $\text{Fe}_2\text{Zr}$  and CuO data and have found that the positions of the nodes depend only weakly on the details of the background subtraction. Typical changes in the node positions when the number of spline knots in the background was varied between one and four, and the  $k$  weight was varied between one and three, were of the order of  $0.01 \text{ \AA}^{-1}$ . This includes even backgrounds which can readily be ruled out by visual inspection, *e.g.* because of a strong low- $r$  peak in the Fourier transforms. It must be noted that the bond distances of all these materials are relatively large (2.5 Å or more), and the analyzed peak in all Fourier transforms was practically independent of the choice of background-subtraction parameters. This will probably not be the case for compounds with shorter bond distances, *e.g.* transition-metal oxides, and the method could exhibit stronger sensitivity to the details of the background subtraction. The  $\text{Fe}_3\text{O}_4$  data were not included in these tests because, as noted above, variations in the position of the nodes cannot be attributed to variations in the background only.

The success of the node-alignment procedure was found to be strongly dependent on the initial guesses for  $R_i$ , although sufficiently accurate initial guesses can usually be obtained, as shown below. In some of the test cases described here, it was not possible to align the nodes with a non-linear method (Levenberg–Marquardt) when the initial guesses were off from the ‘true’ values by as little as  $0.05 \text{ \AA}$ . The reason for this is not yet clear but appears to be related to the extreme sensitivity of the position and number of the nodes in the fitting range on the edge shift  $V_0$  and  $R_i$ . The nodes  $k_{n,i}$  are solutions of the equation

$$2k_{n,i}R_i + \psi_i(k_{n,i}) - \varphi(k_{n,i}) = n_i\pi. \quad (8)$$

Therefore

$$\frac{\partial k_{n,i}}{\partial R_i} = -\frac{2k_{n,i}}{2R_i + \psi'_i(k_{n,i}) - \varphi'(k_{n,i})}, \quad (9a)$$

$$\frac{\partial k_{n,i}}{\partial V_0} = \frac{\alpha}{2k_{n,i}} \frac{2R_i - \varphi'(k_{n,i})}{2R_i + \psi'_i(k_{n,i}) - \varphi'(k_{n,i})}, \quad (9b)$$

where  $\alpha = 2m/\hbar^2$  and the prime denotes a derivative with respect to  $k$ . The Jacobian of the mapping  $V_0, R_i \rightarrow k_{n,i}$  is discontinuous whenever  $2R_i + \psi'_i(k_{n,i}) - \varphi'(k_{n,i}) = 0$  [*i.e.*  $\varphi(k)$  and  $\varphi_i(k)$  have the same slope at  $k = k_{n,i}$ ], in which case small changes in  $V_0$  and  $R_i$  will cause large shifts in the positions of the nodes. This appears to happen most of the time, thus causing the extreme dependence of the solution on the initial guesses, and the high sensitivity of the node-alignment procedure itself. Optimization methods that do not use derivatives explicitly, *e.g.* downhill simplex (Press *et al.*, 1989), failed to converge to within the required accuracy ( $0.002 \text{ \AA}^{-1}$  or less mismatch in the nodes) after more than 500 iterations. However, initial simplex minimization followed by a Levenberg–Marquardt refinement produced accurate results when the initial guesses for  $R_i$  were as much as  $0.15 \text{ \AA}$  off from the ‘true’ values in two out of the three cases discussed here. The results from unrestricted two-shell fits (both for the edge shifts and the bond distances) provided adequate initial guesses in all cases.

At the present time there is no obvious way of extending these results to more complicated (*e.g.* three-subshell) systems, as this would require additional equations for  $A_3, A_4 \dots$ . As expected, and as the CuO example clearly demonstrated, when more than two subshells are present in the EXAFS spectrum the  $\delta\varphi$  method does not give reliable results. However, with a suitable model for the phase corrections it should be possible to apply the method to disordered binary systems. In principle, it should also be possible to use the method to filter multiple-scattering contributions that ‘contaminate’ single-shell data, subject to the ‘small disorder’ requirement and other restrictions outlined above.

## 5. Conclusions

The examples described above show the potential of the  $\delta\varphi$  method for an important class of systems: those with two subshells of atoms with small or ‘Gaussian’ disorder distributed at two unique distances from the central absorber. The advantages over beat analysis, *unrestricted* least-squares fitting and ‘difference’ techniques include (i) improvements in the coordination-number estimates, which can be traced back to the elimination of the strong parameter correlations present in unrestricted multi-shell fits, especially fits involving shells of similar scattering power and phase shifts; (ii) potential for improved spatial resolution with subshells of unlike atoms; and (iii) no external information on the structure of the contributing subshells is required beyond the assumption of small or ‘Gaussian’ disorder.

Further work is needed to understand the sensitive dependence of the outcome of the node-alignment procedure on the initial guesses for the edge shifts and

the bond distances. At the present time it appears that the results from a simultaneous fit of the subshells of interest can provide adequate initial guesses for the edge shifts and bond distances, at least in cases with small disorder.

We would like to thank D. R. Fazzini (IIT) for providing some of the iron-edge EXAFS data used in this paper.

## References

- Bouldin, C., Elam, T. & Furenlid, L. (1995). *Physica B*, **208/209**, 190–192.
- Boyanov, B. I. (1995). PhD thesis, Illinois Institute of Technology, Chicago, IL 60616, USA.
- Bunker, G. (1983). *Nucl. Instrum. Methods*, **A207**, 437–444.
- Bunker, G. (1984). PhD thesis, University of Washington, Seattle, USA.
- Bunker, G. (1988). *Basic Techniques for EXAFS*. Beamline X-9 documentation (National Biostructures PRT). NSLS, Upton, NY, USA.
- Cramer, S. P., Eccles, T. K., Kutzler, F. W., Hodgson, K. O. & Mortenson, L. E. (1976). *J. Am. Chem. Soc.* **98**, 1287–1288.
- McMaster, W. H., Kerr Del Grande, N., Mallett, J. H. & Hubbell, J. H. (1968). *Compilation of X-ray Cross-sections*. UCRL-50174, Section II, Revision I. University of California, USA.
- Martens, G., Rabe, P., Schwertner, N. & Werner, A. (1977). *Phys. Rev. Lett.* **39**, 1411–1414.
- More, J. J., Gabrow, B. S. & Hilstrom, K. E. (1980). *User Guide for MINPACK-1*. Report ANL-80-74. Argonne National Laboratory, USA.
- Press, W. H., Flannery, B. P., Teukolsky, S. A. & Vetterling, W. T. (1989). *Numerical Recipes*. Cambridge University Press.
- Ravel, B. (undated). *UWXAFS Project: ATOMS Software Documentation*. University of Washington Office of Technology Transfer, Seattle, WA, USA.
- Rehr, J. J., Mustre de Leon, J., Zabinsky, S. I. & Albers, R. C. (1991). *J. Am. Chem. Soc.* **113**, 5135–5140.
- Rehr, J. J., Zabinsky, S. I. & Albers, R. C. (1992). *Phys. Rev. Lett.* **69**, 3397–3400.
- Sayers, D. E. & Bunker, B. A. (1988). *X-ray Absorption: Principles, Applications, Techniques of EXAFS, SEXAFS, and XANES*, edited by D. C. Koningsberger & R. Prins, ch. 6. New York: Wiley.
- Sayers, D. E., Stern, E. A. & Lytle, F. W. (1971). *Phys. Rev. Lett.* **27**, 1204–1207.
- Tan, Z., Budnick, J. I. & Heald, S. M. (1989). *Rev. Sci. Instrum.* **60**, 1021–1025.
- Teo, B. K. (1986). *EXAFS: Basic Principles and Data Analysis*, ch. 6, p. 139. Amsterdam: Springer-Verlag.
- Teo, B. K., Eisenberger, P., Reed, J., Barton, J. K. & Lippard, S. J. (1978). *J. Am. Chem. Soc.* **100**, 3225–3228.
- Wyckoff, R. W. G. (1963). *Crystal Structures*, Vols. 1 and 3, 2nd ed. New York: Wiley.